Using carotenoid with ICT state to overcome the limit of photosynthetic light-harvesting

Nao Yukihira
Kwansei Gakuin University
Chiasa Uragami
Kwansei Gakuen University
Kota Horiuchi
Kwansei Gakuen University
Daisuke Kosumi
Kumamoto University https://orcid.org/0000-0001-9339-7913
Alastair Gardiner
Centre ALGATECH https://orcid.org/0000-0001-6161-2914
Richard Cogdell
University of Glasgow https://orcid.org/0000-0003-2119-6607
Hideki Hashimoto (hideki-hassy@kwansei.ac.jp)
Kwansei Gakuin University https://orcid.org/0000-0001-6858-9729

Article

Keywords: Purple Photosynthetic Bacteria, Light-Harvesting Complex, Reconstitution, Carotenoid,Time-Resolved Absorption Spectroscopy, Excitation energy transfer, Intramolecular Charge-Transfer

Posted Date: May 4th, 2022

DOI: https://doi.org/10.21203/rs.3.rs-1531772/v1

Version of Record: A version of this preprint was published at Communications Chemistry on October 26th, 2022. See the published version at https://doi.org/10.1038/s42004-022-00749-6.

Using carotenoid with ICT state to overcome the limit of photosynthetic light-harvesting

Nao Yukihira [a,†], Chiasa Uragami [a,†], Kota Horiuchi [a], Daisuke Kosumi [b], Alastair T. Gardiner [c]
Richard J. Cogdell [d], Hideki Hashimoto [a,*]

[a] Department of Applied Chemistry for Environment, Graduate School of Science and Technology, Kwansei Gakuin University, 1 Gakuen-Uegahara, Sanda, Hyogo, 669-1330, Japan

[b] Institute of Industrial Nanomaterials, Kumamoto University, 2-39-1 Kurokami, Chuou-ku, Kumamoto, 860-8555, Japan

[c] Laboratory of Anoxygenic Phototrophs, Centre ALGATECH, Novohradska 237, 379 01 Třeboň, Czech Republic

[d] Institute of Molecular, Cell and Systems Biology, College of Medical, Veterinary and Life Sciences, University of Glasgow, Glasgow G12 8QQ, Scotland, United Kingdom

† NY and CU contribute equally to this work.

* Corresponding author: Hideki Hashimoto, E-mail: hideki-hassy@kwansei.ac.jp

Abstract

The excitation energy transfer (EET) from carotenoid to bacteriochlorophyll *a* (Bchl *a*) has a significant impact in determining the overall efficiency of utilization of the incident solar spectrum of the primary process of bacterial photosynthesis. This can be enhanced when the carotenoid has intramolecular charge-transfer (ICT) character, such as in the light-harvesting systems in marine alga and diatoms. This study provides new insights into the significance of the ICT excited states following incorporation of a higher plant carotenoid, β-apo-8'-carotenal, into the carotenoidless LH1 system from the purple photosynthetic bacterium, *Rhodospirillum rubrum* strain G9+. β-apo-8'-carotenal generates two types of the ICT excited state in the reconstituted LH1 complex there by achieving an efficiency of EET that exceeds that found in the wild-type LH1 complex. The present study demonstrates a strategy of how to go beyond the EET efficiency from carotenoid to Bchl *a*, which has evolved in the bacterial light-harvesting systems. (150 words)

Key words: Purple Photosynthetic Bacteria, Light-Harvesting Complex, Reconstitution, Carotenoid, Time-Resolved Absorption Spectroscopy, Excitation energy transfer, Intramolecular Charge-Transfer

Introduction

The light-harvesting system found in purple photosynthetic bacteria [1] provides one of the best understood examples of photosynthetic light-harvesting. A great number of studies have been carried out on it to investigate the mechanisms of the energy transfer during light harvesting [2,3]. Learning lessons from photosynthetic light-harvesting can provide important information about how to construct efficient and robust light-harvesting systems that can be utilized in 'artificial photosynthesis' [4].

There are two types of light-harvesting (LH) pigment-protein complexes in purple photosynthetic bacteria. The core light-harvesting 1 (LH1) complex surrounds the reaction center (RC), and the peripheral light-harvesting 2 (LH2) complexes surround the LH1-RC core complex [5]. Solar energy that is captured by the LH2 complex is transferred to LH1 and then to the RC with a quantum efficiency of almost unity. A recent Cryo-EM study has described the detailed molecular architecture of the LH1-RC complex from the purple photosynthetic bacterium *Rhodospirillum* (*Rsp.*) *rubrum* strain S1 [6]. This LH1 complex consists of 16 equally spaced α-β subunits forming a ring structure in which the light absorbing pigments, carotenoid (spirilloxanthin) and bacteriochlorophyll *a* (Bchl *a*) molecules are arranged. Bchl *a* has a Soret absorption band in the ultraviolet spectral region, a Q_x absorption band in the red spectral region, and a Q_y absorption band in the near-infrared region. BChl *a* does not absorb strongly in the blue-green spectral region of light, where the intensity of solar radiation distribution is the strongest. Carotenoids have their main absorption bands in this blue-green spectral region, so they can provide an important boost to light-harvesting [7].

Carotenoids found in light harvesting complexes typically consist of a long polyene backbone that has *N* conjugated C=C bonds, where *N* varies between 9 and 13 [8]. There is a close relationship between the number of conjugated double bonds *N* and the efficiency of excitation energy-transfer (EET). The wavelength of light absorbed by carotenoids depends on *N* [9]. As *N* increases, the EET from carotenoid to Bchl *a* tends to become less efficient [10,11] (see Fig. 1). About 90% of the carotenoids that are bound to the native LH1 complex from *Rsp. rubrum* strain S1 are spirilloxanthin (*N*=13), while other minor carotenoids such as rhodovibrin (*N*=12), anhydrorhodovibrin (*N*=12), rhodopin (*N*=11) and lycopene (*N*=11) are also found, depending on the growth conditions [8,12]. In the LH1 complex of *Rsp. rubrum* strain S1, the efficiency of EET from carotenoids to Bchl *a* is 27%. Previous studies have shown that the EET process from carotenoids to Bchl *a* is dominated by energy transfer from the carotenoid S_2 state to the Q_x state of B880 Bchl *a* in the native LH1 complex from *Rsp. rubrum* strain S1[13-17]. On the other hand, Nakagawa et al. reported that the EET efficiency from carotenoid to Bchl *a* can vary from 28 to 65% in the carotenoid-reconstituted (for $N = 13 – 10$) LH1 complex from *Rsp. rubrum* strain S1 [18], while Akahane et al. reported that it varies from 36 to 78% in the carotenoid-reconstituted (for $N = 13 – 9$) LH1 complex from *Rsp. rubrum* strain G9+, a carotenoidless strain [19]. For the carotenoids with shorter conjugation lengths ($N = 10$ and 9), the EET from the S_1 state of carotenoids becomes also active [17], which contributes to an increase in the efficiency of carotenoid to Bchl *a* EET. Furthermore, it can be

seen that the efficiency of EET from carotenoids to Bchl *a* is proportional to the inverse of the number of conjugated double bonds (1/*N*) (see Fig. 1) [20].

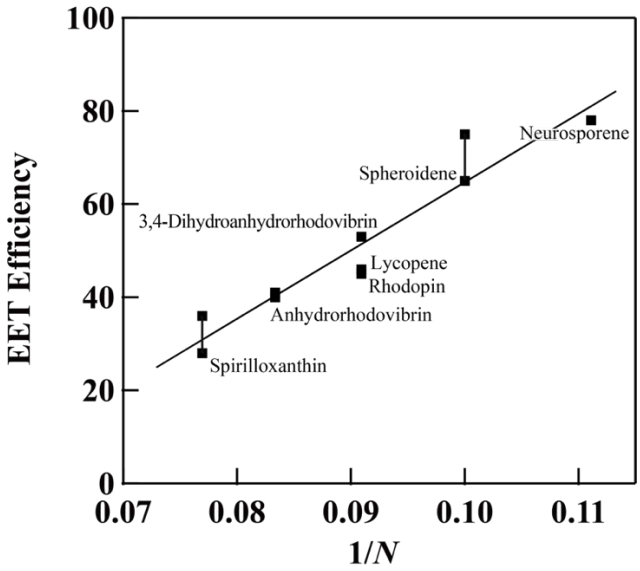

Fig. 1. The relationship between the efficiency of excitation energy transfer from carotenoids to Bchl *a* in the LH1 complex from *Rsp. rubrum* and the inverse of the number of conjugated double bonds (1/*N*) [18,19].

Even though the longer conjugated carotenoids have a lower efficiency of EET they have a superior function in photoprotection [21]. The photoprotective function of carotenoids is mediated by the transfer of triplet-triplet excitation energy from the T_1 state of Bchl *a* to the carotenoid triplet state. Excess light exposure to the LH complexes enhances the production of the T_1 Bchl *a*, which reacts with oxygen to produce singlet oxygen. By scavenging the T_1 Bchl *a* with carotenoid, the generation of singlet oxygen is suppressed, which protects the LH system.

Carotenoids that contain a carbonyl group coupled to their polyene backbone are known to generate an intramolecular charge-transfer (ICT) excited state in a polar environment [22,23]. Following one-photon excitation up to the optically allowed S_2 state, the optically forbidden S_1 state and the ICT state are generated [22,24-26]. The presence of the ICT excited state allows nearly 100% EET from carotenoid to chlorophyll in the LH complexes from algae and diatoms [27-29]. In a previous study, fucoxanthin (see Fig. 2(a)) was successfully incorporated into the LH1 complex from *Rsp. rubrum* strain G9+ [30]. This was remarkable because the algal carotenoid fucoxanthin has a closed end-ring structure and multiple functional groups (allene and carbonyl moieties) in its molecular framework in striking contrast to the relatively simple linear carotenoids, without end-rings, that are always found in the purple bacterial LH systems. However, the EET efficiency from fucoxanthin to Bchl *a* determined by fluorescence excitation spectroscopy was only 28%. However, a femtosecond time-resolved absorption study suggested that the EET efficiency with fucoxanthin in LH1 may be higher than that initially determined because of the presence of a significant pool of inappropriately bound fucoxanthin. In the current investigation, we

have improved the reconstitution methods and have been successful in incorporating a higher plant carotenoid β-apo-8'-carotenal (see Fig. 2(a)) into the LH1 complex from *Rsp. rubrum* strain G9+. The EET efficiency from β-apo-8'-carotenal to Bchl *a* was determined to be 80% by fluorescence excitation spectroscopy, the highest carotenoid to Bchl *a* EET seen in this system so far. Femtosecond time-resolved absorption measurements clearly show that the involvement of the ICT excited state of β-apo-8'-carotenal plays the key role in achieving this efficient EET.

Results and Discussion

1. Reconstitution of β-apo-8'-carotenal into the LH1 complex from *Rsp. rubrum* strain G9+

Fig. 2(b) shows the steady-state absorption spectra of the LH1 complex from the carotenoidless mutant *Rsp. rubrum* strain G9+ together with the reconstituted LH1 complex with β-apo-8'-carotenal (hereafter abbreviated as Reβapo) and β-apo-8'-carotenal. Reβapo shows an absorption band around 400 – 600 nm, which suggests that β-apo-8'-carotenal was incorporated into the carotenoidless LH1. The absorption band of β-apo-8'-carotenal in Reβapo is red-shifted by 3 nm from that in acetone (456 nm → 459 nm). This red-shift is caused by the binding of β-apo-8'-carotenal to LH1 protein. Reβapo has its Q_y absorption maximum at 876 nm. This is shifted to the red by 6 nm in comparison to the carotenoidless LH1 complex (solid blue-line in Fig. 2(b)). The shift of the Q_y absorption maximum reflects the interaction between β-apo-8'-carotenal and B880 Bchl *a* [31]. Previously this shift in the Q_y position has been suggested to reflect the electrostatic interaction between the reconstituted carotenoids and B880 Bchl *a* [18].

Comparison of the intensity of absorbance of the carotenoid absorption region of the native LH1 complex from *Rsp. rubrum* strain S1 (native LH1) and Reβapo shows that in Reβapo it has about half the value seen in the native LH1 (Fig. 2(c)). If we assume that the molar extinction coefficient (ε) of β-apo-8'-carotenal in LH1 is the same as that of spirilloxanthin (*N*=13), it can be estimated that half of the carotenoid binding site is reconstituted with β-apo-8'-carotenal in Reβapo. However, the ε value of β-apo-8'-carotenal is expected to be smaller than that of spirilloxanthin, since the ε of β-apo-8'-carotenal in light petroleum is reported to be 109,800 $mol^{-1}cm^{-1}$ while that of spirilloxanthin in benzene is reported to be 147,200 $mol^{-1}cm^{-1}$ [32, 33]. Therefore, the above estimate probably underestimates the number of the reconstituted carotenoids in Reβapo. Nevertheless, we can safely conclude that at least half of the carotenoid binding sites are occupied in Reβapo.

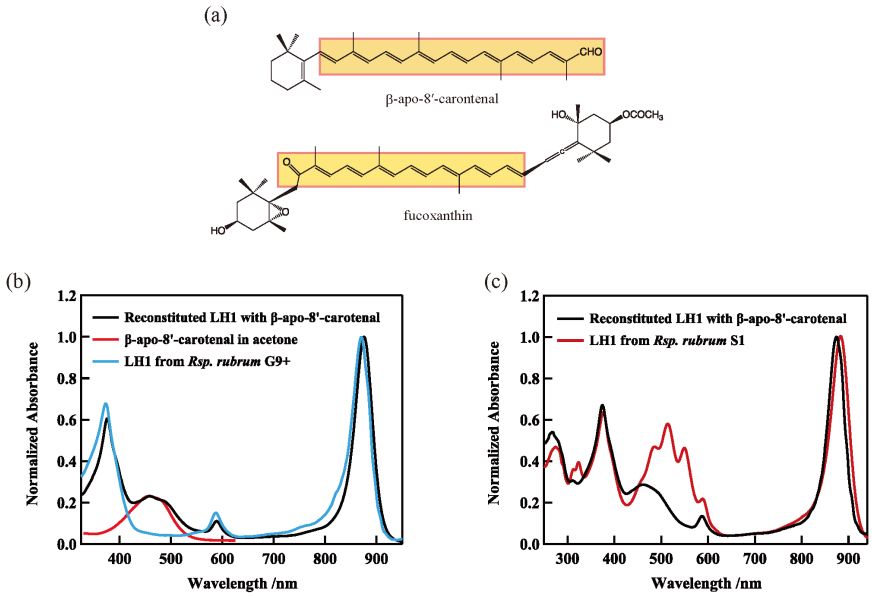

Fig. 2. (a) Chemical structures of β-apo-8'-carotenal and fucoxanthin. Conjugated polyene parts coupled with carbonyl group are highlighted with yellow color. (b) Steady-state absorption spectra of reconstituted LH1 complex from *Rsp. rubrum* strain G9+ with β-apo-8'-carotenal in 20 mM Tris-HCl buffer (pH 8.0) + 0.58% β-OG (solid black line), β-apo-8'-carotenal in acetone (solid red line), and the LH1 complex isolated from *Rsp. rubrum* strain G9+ in 50 mM Phosphate buffer (pH 7.0) + 0.58% β-OG + 10mM sodium ascorbate (solid blue line). (c) Steady-state absorption spectra of reconstituted LH1 complex from *Rsp. rubrum* strain G9+ with β-apo-8'-carotenal in 20 mM Tris-HCl buffer (pH 8.0) + 0.58% β-OG (solid black line), and the LH1 complex isolated from *Rsp. rubrum* strain LH1 in 50 mM Phosphate buffer (pH 7.0) + 0.6% β-OG + 10mM sodium ascorbate (solid red line). Absorption intensity is normalized at B880 maximum. All the measurements were carried out at room temperature.

2. Fluorescence, fluorescence excitation, and 1-T spectra of reconstituted LH1

The EET from carotenoids to B880 Bchl *a* takes place from both the S_2 and S_1 states of the carotenoids [22]. In the case of native LH1 complex from *Rsp. rubrum* strain S1, this process is dominated by the EET from the S_2 state of the carotenoids to the Q_x state of B880 Bchl *a* [13-15,17]. Additional EET from the S_1 state of carotenoids takes place in the LH1 complexes in which shorter conjugated carotenoids were reconstituted [19]. These LH1 complexes with the additional EET pathway show, therefore, higher efficiency of EET from the carotenoids to B880 Bchl *a* (see Table 1). In order to determine the EET efficiency from β-apo-8'-carotenal to B880 Bchl *a* in the present reconstituted LH1 complex, fluorescence emission and excitation spectroscopic measurements were performed. Fig. 3 shows the fluorescence emission, fluorescence excitation and 1 – T spectra of Reβapo, where T is transmittance. The fluorescence emission spectrum was normalized at its intensity maximum. The intense fluorescence signal is observed peaking at 895 nm (solid green-line) when exciting at 500 nm, where β-apo-8'-carotenal primarily absorbs excitation light. Both the fluorescence excitation spectrum monitored at 920 nm and 1 – T spectra were normalized at the Q_y absorption band of B880 Bchl *a*. The intensities at the Q_x and Soret band positions show the coincidence between the fluorescence excitation and 1 – T spectra. This shows that the light energy captured by Q_x or Soret band is transferred to the Q_y

band with 100% efficiency: No backward EET is present from the Q_x state to the S_1/ICT state of β-apo-8'-carotenal [34]. In the $S_0 \rightarrow S_2$ absorption region of β-apo-8'-carotenal (420 - 550 nm), the fluorescence excitation spectrum (solid red-line) is less intense than the corresponding region 1 – T spectrum (solid black-line). Presence of the peak of the carotenoid absorption region in the fluorescence excitation spectrum supports that the EET from β-apo-8'-carotenal to B880 Bchl *a* is taking place. The efficiency of EET from β-apo-8'-carotenal to B880 Bchl *a* can be calculated by the ratio of the fluorescence excitation spectrum divided by the 1 – T spectrum in the carotenoid absorption region (430 – 550 nm) as shown with the solid grey-line in Fig. 3. The average value of the efficiency of EET is 80.0±1.7%, which is significantly higher than that from spirilloxanthin in the wild-type S1 strain of *Rsp. rubrum* (27%) and is also higher than any other reported values of the reconstituted LH1, in which a series of bacterial carotenoids were incorporated (see Table 1). In this way, we have succeeded in creating a reconstituted LH1 complex with the significantly high efficiency of EET from carotenoid to B880 Bchl *a*. However, more importantly as shown below, this turned out to be the underestimate of the true potential that β-apo-8'-carotenal has in Reβapo for the photosynthetic light-harvesting.

Table 1. Summary of the EET efficiency from carotenoid to B880 Bchl *a* in the native and carotenoid-reconstituted LH1 from *Rps. rubrum*.

carotenoid	**N**	**EET(%)**	**reference**
native	13	27	[18]
spirilloxanthin	13	28(36)	[18], ([19])
anhydrorhodovibrin	12	41(40)	[18], ([19])
rhodopin	11	45	[18]
3,4-dihydroanhydrorhodovibrin	11	53	[33]
lycopene	11	45	[19]
spheroidene	10	65(75)	[18], ([19])
neurosporene	9	78	[19]
fucoxanthin	7 + C=O + C=▪=C	28	[29]
β-apo-8'-carotenal	**9 + C=O**	**80**	This study

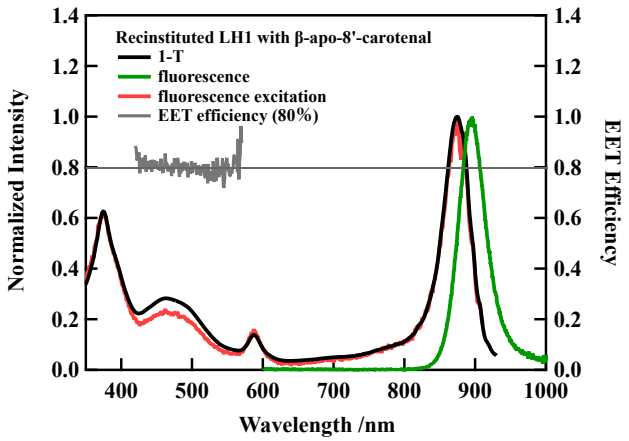

Fig. 3. Steady-state absorption spectrum (solid black line) displayed as 1 – T (Transmission), fluorescence spectrum excited at 500 nm (solid green line), fluorescence excitation spectrum monitored at 920 nm (solid red line), and the efficiency of EET from β-apo-8'-carotenal to B880 Bchl *a* (solid grey line) of the reconstituted LH1 complex from *Rsp. rubrum* strain G9+ with β-apo-8'-carotenal in 20 mM Tris-HCl buffer (pH 8.0) + 0.58% β-OG.

3. Femtosecond time-resolved absorption spectra of the reconstituted LH1

As shown in Fig. 4(b), the femtosecond time-resolved absorption spectrum of β-apo-8'-carotenal recorded at 0.48 ps after excitation in acetone shows a relatively sharp transient absorption band that is ascribable to the $S_1 \rightarrow S_n$ transition in 530 - 580 nm spectral region. It also shows a broad transient absorption that is ascribable to the ICT excited state in 600 – 700 nm spectral region, which shows good agreement with the previous studies [35-38]. Therefore, we tentatively assign these transient absorption bands to the S_1/ICT states. The similar S_1/ICT characteristic transient absorption spectra are also observed in Reβapo recorded at the delay times of 0.5 and 2.0 ps after excitation (see Fig. 4(a)). Therefore, it is clear that the ICT excited state is generated in Reβapo following excitation. As shown in Fig. 4(a), the peak of the '$S_1 \rightarrow S_n$' like absorption band around 550 nm shifts to blue and decays over time. The ratio of the intensities of transient absorption bands originating from the S_1 and ICT states of β-apo-8'-carotenal in Reβapo is similar to those in acetone (Fig. 4(b)). This suggests that the environment in the binding site of β-apo-8'-carotenal in Reβapo as in acetone has a polar character. The near-infrared spectral region transient absorption spectra shown in Fig. 4(a) reflect the photo-induced absorbance change of the Q_y absorption band of B880 Bchl *a*. The bleaching signal of the Q_y absorption band is observed immediately after exciting β-apo-8'-carotenal, the fact which suggests the presence of EET from the S_2 and/or S_1/ICT state of β-apo-8'-carotenal to B880 Bchl *a*. This is because β-apo-8'-carotenal is excited predominantly for femtosecond time-resolved absorption measurements, and hence the immediate bleaching of the Q_y absorption band of B880 Bchl *a* cannot take place without the fast EET from β-apo-8'-carotenal to B880 Bchl *a*.

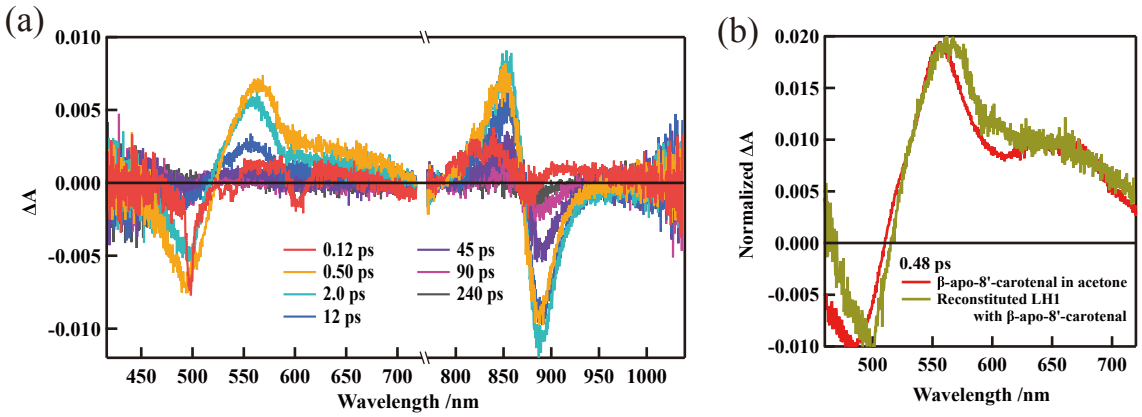

Fig. 4. (a) Femtosecond time-resolved absorption spectra of the reconstituted LH1 with β-apo-8'-carotenal in 20 mM Tris-HCl buffer (pH 8.0) + 0.58% β-OG at room temperature following excitation up to the S_2 state of β-apo-8'-carotenal with 500 nm laser pulse. (b) Femtosecond time-resolved absorption spectra of β-apo-8'-carotenal in acetone (solid red line) and in reconstituted LH1 complex (solid ocher line) recorded at 0.48 ps after excitation. The excitation laser pulse was 500 nm for the reconstituted LH1 and β-apo-8'-carotenal in acetone. All the measurements were carried out at room temperature.

4. Investigation of the relaxation process of the ICT excited states using global and target analyses

In order to a get deeper insight into the excited state relaxations and EET processes in Reβapo, global and target analyses were performed with the complete datasets of the femtosecond time-resolved absorption spectra using a Glotaran program [39,40]. Since the time-resolved absorption spectral measurements were performed independently in the visible (416-718 nm) and near-infrared (767-1036 nm) spectral regions, the spectral analyses were also performed separately in these spectral regions. To begin with, the results in acetone are shown in Fig. 5. The femtosecond time-resolved absorption spectra in the near infrared region are well accounted for using a sequential two components model that have lifetimes of 0.09 ps and 23.8 ps. The former component (solid red-line in Fig. 5(b)) peaking around 900 nm can be assigned to the $S_2 \rightarrow S_n$ transition of β-apo-8'-carotenal in acetone by reference to a previous report [35]. The visible spectral region data were analyzed globally using a sequential model and the result is shown in Fig. 5(a). The visible region data were successfully fitted with three components having lifetimes of 0.09 ps, 0.61 ps and 15.4 ps. For this analysis the 0.09 ps component was fixed since this component has already been assigned to the $S_2 \rightarrow S_n$ transition. The new 0.61 ps component is ascribable to the hot S_1/ICT state, while the 15.4 ps component is ascribable to the S_1/ICT state of β-apo-8'-carotenal in acetone again by reference to the previous report [38]. It is noteworthy here to point out that the spectral pattern of the 15.4 ps EADS (Evolutionally Associated Difference Absorption Spectrum) is composed of a relatively sharp peak around 550 nm, which can be ascribed to the '$S_1 \rightarrow S_n$' like transition, and a broad absorption in the 600 – 700 nm spectral region, which has been used as the evidence of the generation of the ICT excited state. Therefore, we have assigned this 15.4 ps component is originated from a mixed S_1/ICT state [35].

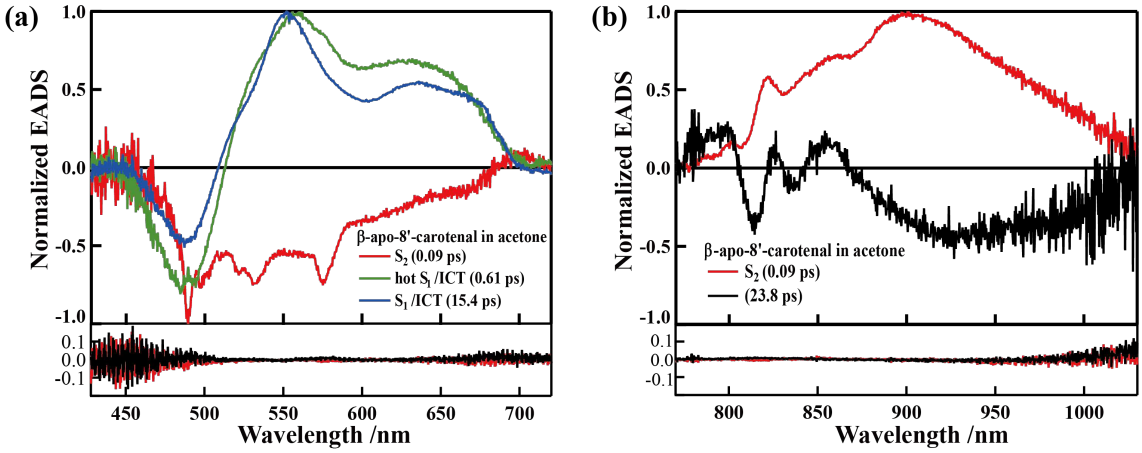

Fig. 5. The results of global analysis based on a sequential model for β-apo-8'-carotenal in acetone in the (a) visible and (b) near-infrared spectral regions. The first (solid black line) and second (solid red line) right singular value vectors of the residual matrix, which corresponds to the residuals of the fittings, is shown at the bottom.

We have also tried to apply a similar global analysis using a sequential model to Reβapo, but without success (see Fig. S1 and S2 in Supplementary Information). To get reliable spectral fitting, a target model, as shown in Fig. 6(b), was necessary. The reason why we constructed this target model is as follows: (1) The ICT excited state of carotenoids with C=O bond in the π-conjugated chain has been proposed to exist in two conformations when they are bound to the LH complexes (blue-form and red-form) [41,42]. (2) The presence of two pools of fucoxanthin, one of which shows EET to B880 Bchl *a* and the other of which does not, has already been found in our previous study for the fucoxanthin reconstituted LH1 complex [30]. When fucoxanthin or peridinin is excited in the low-energy part of the steady-state absorption, it has been reported that there are at least two types of excited states with different charge-transfer characteristics [43-45]. β-apo-8'-carotenal has s-*trans* and s-*cis* conformations of the carbonyl group relative to the polyene-conjugated chain. The s-*trans* carbonyl conformation, which has a high degree of conjugation, is responsible for the generation of the red-form, while the s-*cis* carbonyl conformation is responsible for the blue-form [24,41]. In addition, Pang et al. reported that excitation of β-apo-8'-carotenal at different wavelengths leads to a divided decay from the hot S_2 state to at least two S_1-related states [46].

Fig. 6(a) shows four components of SADS (Species Associated Difference Absorption Spectra) obtained by global fitting using the above-mentioned target model. The first component of the SADS (0.08 ps component, solid black-line) shows a negative change due to ground state bleaching. Therefore, this first SADS component (0.08 ps) is due to the S_2 state. It is unfortunate but we cannot straightforwardly determine the S_2 lifetime from the near infrared spectral region measurement. This is because the spectral changes in the near infrared region reflect the fast dynamics of both the S_2 state of β-apo-8'-carotenal and the Q_x state of B880 Bchl *a* (see Fig. S3 in Supplementary Information). However, the global analysis, assuming the 0.08 ps lifetime for the S_2 β-apo-8'-carotenal, is well reproduced by

the time-resolved absorption signals in the near infrared spectral region (see Fig. S6 in Supplementary Information). The analysis also shows the presence of the EET from the S_2 β-apo-8'-carotenal to the Q_x state of B880 Bchl *a*, since the 0.08 ps S_2 lifetime in Reβapo is shorter than that in acetone (0.09 ps) because of the EET from S_2 β-apo-8'-carotenal to the Q_x B880 Bchl *a*. Again, this is in good support for the assignment of the S_2 lifetime of β-apo-8'-carotenal in Reβapo.

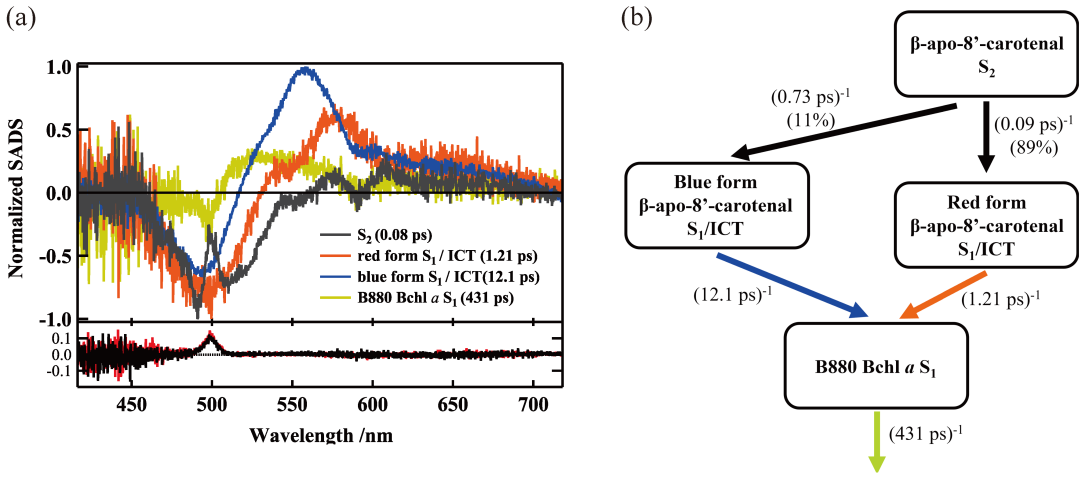

Fig. 6. (a) The result of target analysis applied to the entire observed data set of femtosecond time-resolved absorption spectra of the LH1 complex reconstituted with β-apo-8'-carotenal. The first (solid black line) and second (solid red line) right singular value vectors of the residual matrix, which corresponds to the residuals of the fittings, is shown at the bottom. The peak around 500 nm in the residuals is due to the scattering of the excitation light. Apart from this peak no meaningful spectral pattern is observed in the residuals, a fact which supports the successful spectral fittings. (b) A target model used to analyze the femtosecond time-resolved absorption spectra of Reβapo in the visible spectral region.

The second SADS (1.21 ps component, solid red-line) and the third SADS (12.1 ps component, solid blue-line) in Fig. 6(a) show the characteristic absorption bands that are ascribable to the '$S_1 \rightarrow S_n$' like transition of β-apo-8'-carotenal, respectively, at 575 nm and 550 nm, together with the ICT absorption in 600 – 700 nm spectral region. Therefore, both SADS are thought to be due to the S_1/ICT state. Since the second SADS shows a maximum at a longer wavelength position than the third SADS, we assign the second SADS to the red-form of β-apo-8'-carotenal in Reβapo, while the third SADS to the blue-form of β-apo-8'-carotenal in Reβapo. The possibility to assign the 1.21 ps lifetime component of the second SADS to the vibrationally hot S_1/ICT state can be ruled out, since this component can only be obtained based on the target analysis using the parallel model (see Fig. 6(b)) and the 1.21 ps lifetime is too long to assign the vibrationally hot state. Both the lifetimes of the second (1.21 ps) and the third (12.1 ps) SADS components are shorter than the reported S_1 lifetime (26.2 ps [15] and 26 ps [17]) of β-apo-8'-carotenal in non-polar solvents. This lifetime shortening is caused by the fact the ICT character is expressed when β-apo-8'-carotenal is bound to the LH1 protein: namely, β-apo-8'-carotenal is in the

polar environment when it is bound to Reβapo. Previous reports on peridinin and fucoxanthin when they are bound to Peridinin-Chl *a*-Protein and Fucoxanthin-Chl *a*/*c*-Protein, respectively, also show similar results [27,29,47]. Moreover, overall spectral band shapes of the second and the third SADS are similar to the S_1/ICT transient absorption band of β-apo-8'-carotenal in acetone (see the second EADS in Fig. 5(a)). Therefore, it is suggested that the LH1 bound β-apo-8'-carotenal is in similar polar environment as in acetone.

The fourth SADS (431 ps component, solid ocher-line) in Fig. 6(a) can be due to the S_1 B880 Bchl *a* judging from both the lifetime and the spectral band shape that includes the bleaching of the Q_x absorption band. This idea is further supported by the sub-nanosecond time-resolved absorption measurements as shown later (see section 5). It is interesting to note that the more long-lived triplet component of β-apo-8'-carotenal was not clearly detected in Reβapo in this time regime. This may reflect the efficient singlet-singlet EET from β-apo-8'-carotenal to B880 Bchl *a*. It is reported that the formation of triplet carotenoid is suppressed when carotenoids that show highly efficient singlet-singlet EET to Bchl *a* are reconstituted to the LH system [48].

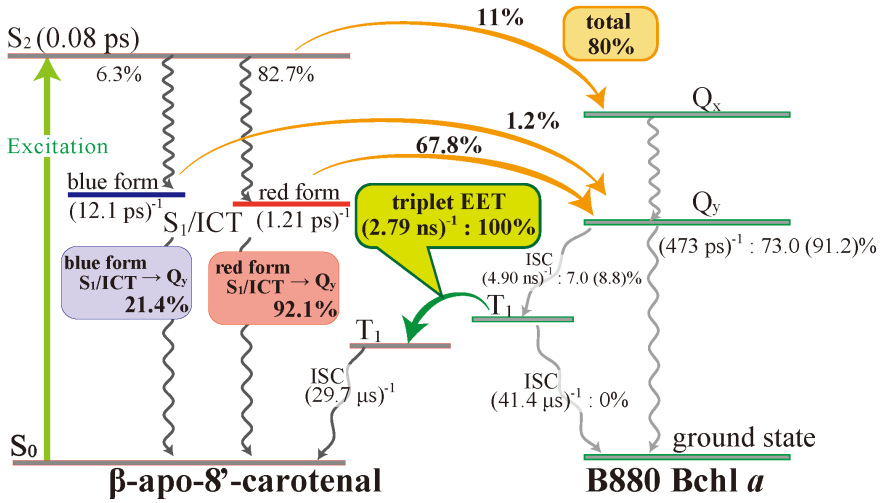

Fig. 7. Schematic illustration of singlet-singlet EET and energy dissipation pathways in Reβapo. Denoted values indicate rates and overall efficiencies (quantum yields). The rate of each process is expressed with the inverse of lifetime. Abbreviation ISC stands for intersystem crossing.

The singlet-singlet EET pathways from β-apo-8'-carotenal to B880 BChl *a* in Reβapo is summarized in Fig. 7. The lifetimes of the S_2 and the two types of S_1/ICT species of β-apo-8'-carotenal in Reβapo are shorter than those in acetone. This finding reflects EET from β-apo-8'-carotenal to B880 Bchl *a* in Reβapo. The efficiency of EET can be calculated from the lifetimes determined by global and target analyses; the following equation (1) was used to calculate the efficiency of singlet-singlet EET (Φ_{EET}) from β-apo-8'-carotenal to B880 Bchl *a*.

$$\Phi_{EET} = \frac{k_{EET}}{k_{IC} + k_{EET}} \times 100\ (\%) \qquad (1).$$

In the reconstituted LH1 complex, k_{EET} is the rate for the components involved in the EET processes, $S_2 \rightarrow Q_x$ or S_1/ICT $\rightarrow Q_y$ (see Fig. 7). k_{IC} is the rate for the internal conversion of β-apo-8'-carotenal from the $S_2 \rightarrow S_1$/ICT or S_1/ICT $\rightarrow S_0$ of β-apo-8'-carotenal in acetone. Here, the contribution of the radiative rate constant is omitted since the fluorescence of β-apo-8'-carotenal is negligible.

The S_2 lifetime of β-apo-8'-carotenal in acetone was determined to be 0.09 ps (k_{IC} = (0.09 ps)$^{-1}$), while that in Reβapo is 0.08 ps ($k_{IC} + k_{EET}$ = (0.08 ps)$^{-1}$). Therefore, the efficiency of EET from the S_2 β-apo-8'-carotenal to Q_x B880 Bchl *a* was calculated to be 11%. The S_1/ICT lifetime of β-apo-8'-carotenal in acetone is 15.4 ps (k_{IC} = (15.4 ps)$^{-1}$). The S_1/ICT lifetime of the red-form β-apo-8'-carotenal in Reβapo is 1.21 ps ($k_{IC} + k_{EET}$ = (1.21 ps)$^{-1}$), while that of the blue-form is 12.1 ps ($k_{IC} + k_{EET}$ = (12.1 ps)$^{-1}$). Therefore, the efficiency of EET from the red-form S_1/ICT to Q_y of B880 Bchl *a* is calculated to be 92.1% and that from the blue-form S_1/ICT is calculated to be 21.4%. This result suggests that the EET from the red-form S_1/ICT state is superior to that from the blue-form S_1/ICT state. Since the total efficiency of EET from β-apo-8'-carotenal to B880 Bchl *a* calculated from the absorption and fluorescence excitation spectra was 80%, the ratio of energy relaxation from the S_2 state to the red-form S_1/ICT and blue-form S_1/ICT states are 82.7% and 6.3%, respectively (see Supplementary Information). The results of the target analysis shown in Fig. 7 were the ones that were finally optimized by incorporating this ratio of relaxation from the S_2 state to the two-components (red-form and blue-form) of the S_1/ICT states (82.7% and 6.3%). In the red-form S_1/ICT state, the efficiency of EET from β-apo-8'-carotenal to B880 Bchl *a* turned out to be as high as 92.1%, which is much higher than that of the wild-type LH1 complexes and shows the highest value among the carotenoid reconstituted LH1 complexes.

It has been found that the effective number of conjugated double bonds (N_{eff}) can be calculated from the 0-0 transition energy of the steady-state absorption spectrum of carotenoids in *n*-hexane solution [49]. The maximum wavelength of the 0-0 transition of β-apo-8'-carotenal in *n*-hexane is 481 nm (20,790 cm^{-1} in energy), which corresponds to N_{eff} = 9.8 (see Fig. S4 in Supplementary Information). Compared to the linear carotenoid spheroidene (N = 10), N_{eff} of β-apo-8'-carotenal is slightly shorter. The efficiency of EET from spheroidene to B880 Bchl *a* is reported to be 65-75%[18,19]. The total EET efficiency from β-apo-8'-carotenal to B880 Bchl *a* was determined to be 80%, which is slightly higher than the case of spheroidene. This result can be well accounted for if we adopt the N_{eff} value of β-apo-8'-carotenal, which is slightly smaller than that of spheroidene (N = 10). However, the efficiency of EET from neurosporene (N = 9) is reported to be 78%, the amount of which is almost equivalent to or just less than the case of β-apo-8'-carotenal. This remarkable result cannot be explained based on the simple consideration of N_{eff} of β-apo-8'-carotenal, since N_{eff} of β-apo-8'-carotenal is larger than N of neurosporene. Surprisingly, the efficiency of EET from the red-form S_1/ICT to B880 BChl *a* was even higher (92.1%), suggesting that the involvement of the S_1/ICT state plays a key role in the achievement of the highly efficient EET (see

Fig. 8).

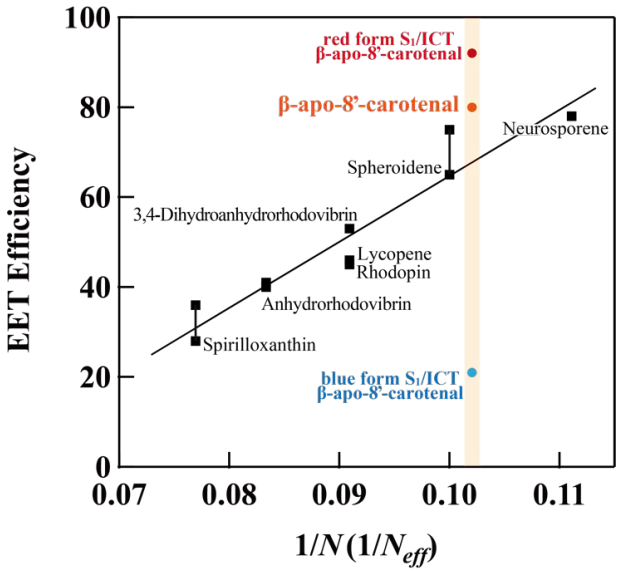

Fig. 8. The relationship between the efficiency of EET from carotenoids to Bchl *a* in Reβapo and the inverse of the number of conjugated double bonds ($1/N$) or the inverse of the effective number of conjugated double bonds ($1/N_{eff}$).

The EET from S_1/ICT was found to be dominant when compared the EET efficiency from S_2. This finding is quite unusual in the case of bacterial light-harvesting systems, although similar trend has already been found in the LH complexes from algae and diatoms. The slow onset of Q_y bleaching signal of B880 Bchl *a*, found also in the present study, support the EET pathway from the S_1/ICT sate of β-apo-8'-carotenal to the Q_y state of B880 Bchl *a* being present (see Fig. S5 in Supplementary Information). This trend is clearly different from the previous reports for the LH1 complex in which the EET from the S_2 state of carotenoids to the Q_x state of B880 Bchl *a* is the dominant one [13-17]. The predominant EET pathway from S_1/ICT to Q_y is presumably due to the coupling of the ICT excited state to the S_1 state. Recently, Marcolin et al. reported that the ICT state is strongly bound to the S_2 state in fucoxanthin in polar organic solvents [50]. This finding is consistent with our previous results using Stark absorption spectroscopy [42]. However, the present observation is different from those of Marcolin et al., because the 0-0 band of the S_0-S_2 transition is clearly photoexcited in this study; Macrolin et al. excited the long wavelength edge of the $S_0 \rightarrow S_2$ transition of fucoxanthin because of the limitation of the pump spectrum. In other words, we can propose that the S_1 state, which is originally an additional EET channel of the EET to B880 Bchl *a*, is elevated to a major EET channel by the coupling with the ICT excited state to form S_1/ICT [27].

There is an opposite view that claims the ICT state has little effect on the EET efficiency based on a study on LH1 from a different species of photosynthetic bacterium that contains spheroidenone (a carbonyl containing carotenoid) as a major carotenoid [51]. However, our present study clearly shows that this may not always be true.

5. Sub-nanosecond time-resolved absorption spectroscopy on Reβapo

Finally, we would like to address whether β-apo-8'-carotenal in Reβapo is photoprotective or not. It is always important to make sure the presence of the photoprotective function of carotenoid in the reconstituted LH system in order to guarantee the robustness of the system. To this end, sub-nanosecond time-resolved absorption spectroscopy has been applied to Reβapo. Fig. 9 shows the results of the global analysis based on a 3-components sequential model using the entire observed dataset of the sub-nanosecond time-resolved absorption spectra of Reβapo. The first EADS (431 ps component) shown with solid black-line in Fig. 9 can be assigned to the S_1 state of B880 Bchl *a*. The lifetime of this component was fixed so as to agree with the longest lifetime component (the 481 ps component) that has been determined by the femtosecond time-resolved absorption spectroscopy shown before (see section 4). The spectral band shape in the 500 - 600 nm region of the first EADS agrees well with that of the 481 ps component determined by the femtosecond time-resolved absorption spectroscopy (see the solid ocher-line in Fig. 6(a)), a fact which supports the validity of this protocol. The second EADS (2.79 ns component) shown with solid red-line in Fig. 9 can be assigned to the T_1 state of B880 Bchl *a* judging from both the spectral shape and the lifetime. The third EADS (29.7 μs component) shown with solid blue-line can undoubtedly be assigned to the T_1 state of β-apo-8'-carotenal in Reβapo judging from the spectral peak around 530 nm and the lifetime, although the spectral amplitude is very low and hence the spectrum becomes noisy.

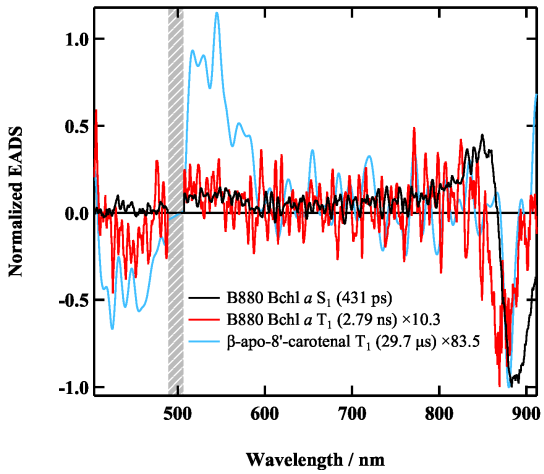

Fig. 9. EADS obtained by the global analysis against the entire observed dataset of nanosecond time-resolved absorption spectra of Reβapo based on a 3-components sequential model. The hatched bar at 500 nm shows the region of pump laser light. The spectra were truncated at this pump laser spectral region to reduce the effect of the pump light scattering.

As shown in Fig. 7, the singlet excitation-energy transferred from β-apo-8'-carotenal to B880 Bchl *a* in Reβapo is dissipated from the Q_y state of B880 Bchl *a* both radiatively and non-radiatively. During this dissipation process, a part of the Q_y (S_1) state of B880 Bchl *a* transforms to the T_1 state by

intersystem crossing. How much of the S_1 B880 Bchl *a* transforms to the T_1 state can be calculated using the amplitude of the first and second EADS shown in Fig. 9 (see Supplementary Information for the details of the calculation). It turned out that the 8.9% of the S_1 B880 Bchl *a* transforms to the T_1 B880 Bchl *a*, and 91.1% of the S_1 energy of B880 Bchl *a* is dissipated by radiative and non-radiative relaxation. It is noteworthy here that this 8.9% efficiency of triplet-triplet energy transfer shows good agreement with the result (8%) of the LH2 complex from *Rhodobacter sphaeroides* strain 2.4.1 [52]. This T_1 B880 Bchl *a* decays with the rate of $(2.79\ \text{ns})^{-1}$ through the processes of both triplet-triplet EET to β-apo-8'-carotenal and intersystem crossing. The T_1 β-apo-8'-carotenal dissipates its triplet energy harmlessly as heat to the surrounding environment with the rate of $(29.7\ \mu\text{s})^{-1}$. According to our previous study on the carotenoidless LH1 complex from *Rsp. rubrum* strain G9+ [34], the rate of the intersystem crossing of the T_1 B880 Bchl *a* to go back to the ground state was determined to be $(41.4\ \mu\text{s})^{-1}$. Therefore, the efficiency (Φ_{EET}^{T}) of triplet-triplet energy transfer from T_1 B880 Bchl *a* to β-apo-8'-carotenal can be calculated according to the following equation (2).

$$\Phi_{EET}^{\mathrm{T}} = \frac{k_{EET}^{\mathrm{T}}}{k_{ISC} + k_{EET}^{\mathrm{T}}} \times 100\ (\%) \qquad (2).$$

Here, k_{ISC} is the rate of intersystem crossing of T_1 B880 Bchl *a* ($k_{ISC} = (41.4\ \mu s)^{-1}$) and k_{EET}^{T} is the rate of triplet-triplet energy transfer from T_1 B880 Bchl *a* to β-apo-8'-carotenal. Since $k_{ISC} + k_{EET}^{\mathrm{T}} = (2.79\ ns)^{-1}$ has been determined by sub-nanosecond time-resolved absorption spectroscopy, Φ_{EET}^{T} can be calculated to be 100%. Therefore, this clear result shows that photoprotection by β-apo-8'-carotenal in Reβapo is fully functional.

Conclusion

The present study provides new insights into the role of the ICT excited states of carotenoids by successfully incorporating a higher plant carotenoid, β-apo-8'-carotenal, to the carotenoidless LH1 system from a purple photosynthetic bacterium, *Rsp. rubrum* strain G9+. Importantly, the EET from the S_1/ICT state to B880 Bchl *a* is the major channel in Reβapo. It is clear that the ICT state plays a key role in the realization of highly efficient EET from carotenoid to Bchl *a*. Reβapo is robust since the photoprotective mechanism of β-apo-8'-carotenal is fully functional. The present study clearly suggests a strategy of how to go beyond the currently available EET efficiency from carotenoid to Bchl *a* by harnessing the properties of ICT states.

Experimental Section

Cell growth and preparation of chromatophores

Cells of *Rsp. rubrum* strain G9+ (a carotenoidless mutant) were photosynthetically grown under anaerobic conditions with C-succinate medium modified from Cohen-Bazire *et al*. at 27 °C [53]. The cells were harvested by centrifugation (18,800g × 10 min at 4 °C), resuspended in 20 mM MES buffer (pH 7.0), and stored in a freezer (–30 °C) until use. Chromatophores of *Rsp. rubrum* strain G9+ were prepared as described previously [54].

Isolation and purification of B820 heterodimers from the native LH1 complex from *Rsp. rubrum* strain G9+

The native LH1 complex without carotenoid was isolated from the freshly prepared chromatophores of *Rsp. rubrum* strain G9+ according to the reported protocols [55,56]. The B820 heterodimers were isolated from the native LH1 complex as described previously [57-59] following solubilization with 1.2% octyl-β-glucopyranoside (β-OG) in 50 mM phosphate buffer (pH 7.0) with the presence of 10 mM sodium ascorbate. The B820 heterodimers were further purified by means of sucrose density gradient (0.6 – 0.8 M) ultracentrifugation (165, 000g × 16 hrs. at 4°C) and stored in the freezer (–30 °C) until required.

Reconstitution of β-apo-8'-carotenal into the LH1 complex

The reconstitution of carotenoid into the LH1 complex was performed using the reported method by Yukihira et al.[30] with a slight modification. All-*trans*-β-apo-8′-carotenal were purchased from Sigma-Aldrich and used without further purification. The acetone solution of β-apo-8'-carotenal (OD_{456} = 1.2) was very slowly dropped, under vigorous flow of N_2 gas, into a 50 mM phosphate buffer (pH 7.0) solution of B820 (OD_{820} = 6-8) containing 1.2% β-OG at room temperature. β-apo-8'-carotenal was added until its absorbance band became three times as large as that of the Q_x absorption band of Bchl *a*. The solution was then diluted with the same volume of 50 mM phosphate buffer (pH 7.0) with 10 mM sodium ascorbate so that the final concentration of β-OG becomes 0.6%. This procedure (dilution of the detergent concentration) induced the reassembly of the B820 heterodimers to form the LH1 ring structure [56]. During this process β-apo-8'-carotenal was incorporated into the LH1 complex. Following the reconstitution of the LH1 complex which contains excess amount of carotenoid, the reconstituted LH1 complex was further purified by ion-exchange chromatography, using DEAE-cellulose (DE52, Whatman) as a fixed phase. The reconstituted LH1 complex was charged to the DE52 column (1.5 cm i.d.) pre-equilibrated by 20 mM Tris-HCl buffer (pH 8.0) containing 0.58% β-OG. Excess carotenoids were eluted in 20 mM Tris-HCl buffer (pH 8.0) containing 0.58% β-OG and 50 mM NaCl, and the reconstituted LH1 complex was eluted using 20 mM Tris-HCl buffer (pH 8.0) containing 0.58% β-OG and 500 mM NaCl.

Steady-state spectroscopic measurements

Steady-state absorption spectral measurements were performed using a JASCO V-730 UV-vis spectrophotometer. Fluorescence emission and excitation spectra of the reconstituted LH1 complexes (OD_{876} = 0.3) were recorded with a HORIBA Duetta spectrofluorometer using a 1 cm optical path-length quartz cuvette at room temperature. The fluorescence-excitation spectra were detected at 920 nm which corresponds to the emission from the B880 absorption band. The efficiency of EET from β-apo-8'-carotenal to Bchl *a* in the LH1 complexes was determined by comparing the fluorescence excitation spectra with the fractional absorption (1 – T) spectra normalizing at the peak of the Q_y transition of B880 Bchl *a*. The 1-T spectra were measured by HORIBA Duetta for the purpose of accurate comparison of the fluorescence excitation and 1- T spectra.

Femtosecond time-resolved absorption measurements

A part of the output pulses from a femtosecond Ti:Sapphire regenerative amplifier (Spectra Physics, Solstice Ace, 80 fs pulse duration, 3.5 mJ/pulse (3.5 W), 1 kHz repetition) were guided to excite an optical parametric amplifier (Spectra Physics, TOPAS-Prime) and a wavelength converter (Spectra Physics, NirUVis) to generate pump pulses. The excitation pulse at 500 nm used to excite the $S_0 \rightarrow S_2$ absorption band of β-apo-8'-carotenal was generated with this set-up. The excitation intensity was set to 20 nJ/pulse and the beam was focused on to the sample with a diameter of 200 μm. Another small part of the output from a femtosecond Ti:Sapphire regenerative amplifier (80 fs pulse duration, 100 μJ/pulse (100 mW), 1 kHz repetition) were guided to a sapphire plate after passing through a rotational neutral density filter to generate probe super-continuum pulses using a nonlinear optical process of self-phase modulation. A sapphire plate of 2 mm thickness was used to generate the probe pulses when recording the transient absorption spectra in the visible spectral region from 430 – 720 nm, while that with 7 mm thickness is used when recording the transient absorption spectra in the near infrared spectral region from 770 – 1036 nm. The diameter of the probe beam was 250 μm at the sample position. To avoid unnecessary confusion caused by the anisotropy, we chose the magic angle (54.7°) configuration for the polarization between the pump and probe pulses. The probe pulses were irradiated to the sample with 1 kHz repetition rate, while the repetition rate of the pump pulses was reduced to 500 Hz using an optical chopper (Terahertz Technologies Inc., C-995 Optical Chopper) synchronously operated with the 1 kHz output signal from the oscillator of the femtosecond regenerative amplifier. The probe pulses that passed through the sample is collected by a spectrometer (Acton Research Corporation, SpectraPro 275) after passing through a Glan-Thompson prism and the spectral dataset was recorded by a 1024-channel multichannel photodiode detector (Hamamatsu, Linear image sensor S3903-1024Q mounted on linear image sensor driving circuit C7884).

The sample was placed in a static quartz cuvette that had an optical path-length of 2 mm. The solution inside the cuvette was continuously stirred using a micro stirrer bar during the measurements. The optical density of the sample was set to be 0.2-0.3 at the excitation wavelength. The integrity of the sample was checked by comparison of the steady-state absorption spectra of the sample before and after the measurements. All the time-resolved measurements were performed at room temperature.

Sub-nanosecond time-resolved absorption measurements

Sub-nanosecond pump-probe spectroscopic measurements were performed using a combination of a Ti:Sapphire regenerative amplifier (Hurricane-X, Spectra Physics, 100 fs pulse duration at 800 nm) and a sub-ns pump-probe time-resolved absorption spectrophotometry system (EOS Vis-Nir, Ultrafast Systems) [52,60]. Excitation pulses at 500 nm was prepared through the second harmonic generation of the output of an optical parametric amplifier (OPA-800 CF, Spectra Physics). The excitation intensity was set to 20 nJ/pulse with a pulse width of 100 fs and a beam diameter of 200 μm. The time delay between the pump and probe pulses was adjusted electronically (Ultrafast Systems, EOS). All the measurements were performed at room temperature. The instrumental response function of the system was estimated to be approximately 500 ps, which corresponded to the pulse width of the probe super-continuum light; however, the pump light was as short as 100 fs.

Acknowledgements

N.Y. thanks the financial support from JSPS KAKENHI for JSPS fellowship for junior researcher (No. 20J10152). HH thanks JSPS KAKENHI, Grant-in-Aids for Basic Research (B) (No. 16H04181) for financial support. HH and DK are grateful to JSPS KAKENHI, Scientific Research on Innovative Areas “Innovations for Light-Energy Conversion (I^4LEC)” (No.17H06433, No. 17H06437 & No. 18H05173) by JSPS for financial support. ATG was funded by the Czech Science Foundation project PhotoGemm+ 19-28778. R.J.C. gratefully acknowledge support from the Photosynthetic Antenna Research Center, an Energy Frontier Research Center funded by the U.S. Department of Energy, Office of Science, Office of Basic Energy Sciences under Award Number DE-SC 0001035.

Author contributions

N.Y. made all the samples, performed the steady-state spectroscopy measurements, analyzed the time-resolved absorption data, and drafted the original manuscript. C.U. performed all the time-resolved measurements and analyzed the data. K.H. and D.K. manipulated the time-resolved absorption measurements and contributed to set up the time-resolved absorption spectroscopy system. A.T.G.

supervised the sample preparation. R.J.C. contributed to supervise the sample preparation and interpretation of the results and revised the manuscript. H.H. conceptualized this work, supervised the work of N.Y., K.H. and C.U., contributed to analyze the spectral data, and revised the original and revised drafts of the manuscript. All authors contributed to revise the manuscript.

Data Availability

The data that support the findings of this study are available from the authors on reasonable request.

Competing interests

The authors declare that they have no known competing financial interests or personal relationships that could have appeared to influence the work reported in this paper.

Additional information

Supplementary information

Supplementary information related to this article can be found, in the online version.

References

1 Green, B. R. & Parson, W. W. *Light-Harvesting Antennas in Photosynthesis* (Kluwer Academic Publishers, Dordrecht, 2003).

2 Hashimoto, H., Sugai, Y., Uragami, C., Gardiner, A. T. & Cogdell, R. J. Natural and artificial light-harvesting systems utilizing the functions of carotenoids. *J. Photochem. Photobiol. C* **25**, 46-70 (2015).

3 Hunter, C. N., Daldal, F., Thurnauer, M. C. & Beatty, J. T. *The Purple Phototrophic Bacteria* (Springer, Dordrecht, 2009).

4 Cogdell, R. J., Gardiner, A. T., Yukihira, N. & Hashimoto, H. Solar fuels and inspiration from photosynthesis. *J. Photochem. Photobiol. A* **353**, 645-653 (2018).

5 Blankenship, R. E., Madigan, M. T. & Bauer, C. E. *Anoxygenic photosynthetic bacteria* (Kluwer Academic Publishers, Dordrecht, 1995).

6 Tani, K. et al. Cryo-EM Structure of the Photosynthetic LH1-RC Complex from *Rhodospirillum rubrum*. *Biochem.* 2483-2491 (2021).

7 Hashimoto, H., Uragami, C. & Cogdell, R. J. *Carotenoids in Nature Ch. 4* (Springer, Dordrecht, 2016).

8 Qian, P. et al. Time-dependent changes in the carotenoid composition and preferential binding of spirilloxanthin to the reaction center and anhydrorhodovibrin to the LH1 antenna complex in *Rhodobium marinum*. *Photochem. Photobiol.* **74**, 444-452 (2001).

9 Kosumi, D. et al. The dependence of the ultrafast relaxation kinetics of the S_2 and S_1 states in β-carotene homologs and lycopene on conjugation length studied by femtosecond time-resolved absorption and Kerr-gate fluorescence spectroscopies. *J. Chem. Phys.* **130**, 214506 (2009).

10 Frank, H. A. et al. Carotenoid-to-bacteriochlorophyll singlet energy transfer in carotenoid-incorporated B850 light-harvesting complexes of *Rhodobacter sphaeroides* R-26.1. *Photochem. Photobiol.* **57**, 49-55 (1993).

11 Desamero, R. Z. B. et al. Mechanism of energy transfer from carotenoids to bacteriochlorophyll: Light-harvesting by carotenoids having different extents of π-electron conjugation incorporated into the B850 antenna complex from the carotenoidless bacterium *Rhodobacter sphaeroides* R-26.1. *J. Phys. Chem. B* **102**, 8151-8162 (1998).

12 Naruse, M., Hashimoto, H., Kuki, M. & Koyama, Y. Triplet excitation of precursors of spirilloxanthin bound to the chromatophores of *Rhodospirillum rubrum* as detected by transient Raman spectroscopy. *J. Mol. Struct.* **242**, 15-26 (1991).

13 Gradinaru, C. C. et al. An unusual pathway of excitation energy deactivation in carotenoids: singlet-to-triplet conversion on an ultrafast timescale in a photosynthetic antenna. *Proc. Natl. Acad. Sci. USA* **98**, 2364-2369 (2001).

14 Papagiannakis, E. et al. A near-infrared transient absorption study of the excited-state dynamics of the carotenoid spirilloxanthin in solution and in the LH1 complex of *Rhodospirillum rubrum*. *J. Phys. Chem. B* **107**, 11216-11223 (2003).

15 Rondonuwu, F. S., Watanabe, Y., Fujii, R. & Koyama, Y. A first detection of singlet to triplet conversion from the $1^1B_u^-$ to the 1^3A_g state and triplet internal conversion from the 1^3A_g to the 1^3B_u state in carotenoids: dependence on the conjugation length. *Chem. Phys. Lett.* **376**, 292-301 (2003).

16 Koyama, Y. & Kakitani, Y. *Chlorophylls and Bacteriochlorophylls* Ch.30 (Springer, Dordrecht, 2006).

17 Kosumi, D. et al. Ultrafast energy-transfer pathway in a purple-bacterial photosynthetic core antenna, as revealed by femtosecond time-resolved spectroscopy. *Angew. Chem. Int. Ed.* **50**, 1097-1100 (2011).

18 Nakagawa, K. et al. Probing the effect of the binding site on the electrostatic behavior of a series of carotenoids reconstituted into the light-harvesting 1 complex from purple photosynthetic bacterium *Rhodospirillum rubrum* detected by Stark spectroscopy. *J. Phys. Chem. B* **112**, 9467-9475 (2008).

19 Akahane, J., Rondonuwu, F. S., Fiedor, L., Watanabe, Y. & Koyama, Y. Dependence of singlet-energy transfer on the conjugation length of carotenoids reconstituted into the LH1 complex from *Rhodospirillum rubrum* G9. *Chem. Phys. Lett.* **393**, 184-191 (2004).

20 Yamamoto, M. et al. Reassociation of all-*trans*-3,4-dihydroanhydrorhodovibrin with LH1 subunits isolated from *Rhodospirillum rubrum*: Selective binding of all-*trans* isomer from mixture of *cis*- and *trans*-isomers. *B. Chem. Soc. JPN* **86**, 121-128 (2013).

21 Kakitani, Y. et al. Selective binding of carotenoids with a shorter conjugated chain to the LH2 antenna complex and those with a longer conjugated chain to the reaction center from *Rubrivivax gelatinosus*. *Biochemistry* **46**, 7302-7313 (2007).

22 Hashimoto, H., Uragami, C., Yukihira, N., Gardiner, A. T. & Cogdell, R. J. Understanding/unravelling carotenoid excited singlet states. *J. R. Soc. Interface* **15**, 20180026 (2018).

23 Polívka, T. & Sundström, V. Ultrafast dynamics of carotenoids excited states - From solution to natural

and artificial systems. *Chem. Rev.* **104**, 2021-2071 (2004).

24 Kosumi, D. et al. Characterization of the intramolecular transfer state of marine carotenoid fucoxanthin by femtosecond pump–probe spectroscopy. *Photosynth. Res.* **121**, 61-68 (2014)

25 Kosumi, D. et al. One- and two-photon pump–probe optical spectroscopic measurements reveal the S_1 and intramolecular charge transfer states are distinct in fucoxanthin. *Chem. Phys. Lett.* **483**, 95-100 (2009).

26 Cogdell, R. J. & Frank, H. A. How carotenoids function in photosynthetic bacteria. *Biochim. Biophys. Acta* **895**, 63-79 (1987).

27 Kosumi, D. et al. Excitation energy-transfer dynamics of brown algal photosynthetic antennas. *J. Phys. Chem. Lett.* **3**, 2659-2664 (2012).

28 Wagner, N. L., Greco, J. A., Enriquez, M. M., Frank, H. A. & Birge, R. R. The nature of the intramolecular charge transfer state in peridinin. *Biophys. J.* **104**, 1314-1325 (2013).

29 Zigmantas, D., Hiller, R. G., Sundström, V. & Polívka, T. Carotenoid to chlorophyll energy transfer in the peridinin-chlorophyll-*a*-protein complex involves an intramolecular charge transfer state. *Proc. Natl. Acad. Sci. USA* **99**, 16760-16765 (2002).

30 Yukihira, N. et al. Strategies to enhance the excitation energy-transfer efficiency in a light-harvesting system using the intra-molecular charge transfer character of carotenoids. *Faraday Discuss.* **198**, 59-71 (2017).

31 Nakagawa, K. et al. Probing binding site of bacteriochlorophyll *a* and carotenoid in the reconstituted LH1 complex from *Rhodospirillum rubrum* S1 by Stark spectroscopy. *Photosynth. Res.* **95**, 339-344 (2008).

32 Britton, G. *Carotenoids Volume 1B: Spectroscopy Ch.2* (Birkhauser Verlag, Basel, 1995).

33 Wang, X.-F. et al. Effects of plant carotenoid spacers on the performance of a dye-sensitized solar cell using a chlorophyll derivative: Enhancement of photocurrent determined by one electron-oxidation potential of each carotenoid. *Chem. Phys. Lett.* **423**, 470-475(2006).

34 Uragami, C. et al. Photoprotective mechanisms in the core LH1 antenna pigment-protein complex from the purple photosynthetic bacterium, *Rhodospirillum rubrum*. *J. Photochem. Photobiol. A* **400**, 112628 (2020).

35 Ragnoni, E., Di Donato, M., Iagatti, A., Lapini, A. & Righini, R. Mechanism of the intramolecular charge transfer state formation in all-*trans*-β-apo-8'-carotenal: influence of solvent polarity and polarizability. *J. Phys. Chem. B* **119**, 420-432 (2015).

36 Zhang, L. Femtosecond time-resolved difference absorption spectroscopy of all-*trans*-β-Apo-8'-carotenal. *Sci. China Ser. G* **47**, 208-222 (2004).

37 Durchan, M., Fuciman, M., Slouf, V., Kesan, G. & Polivka, T. Excited-state dynamics of monomeric and aggregated carotenoid 8 '-Apo-b-carotenal. *J. Phys. Chem. A* **116**, 12330-12338 (2012).

38 Kopczynski, M., Ehlers, F., Lenzer, T. & Oum, K. Evidence for an Intramolecular Charge Transfer State in 12'-Apo-β-caroten-12'-al and 8'-Apo-β-caroten-8'-al: Influence of Solvent Polarity and Temperature. *J. Phys. Chem. A* **111**, 5370-5381 (2007).

39 van Stokkum, I. H. M., Larsen, D. S. & van Grondelle, R. Global and target analysis of time-resolved spectra. *Biochim. Biophys. Acta* **1657**, 82-104 (2004).

40 Snellenburg, J. J., Laptenok, S. P., Seger, R., Mullen, K. M. & Stokkum, I. H. M. v. Glotaran: A Java-Based Graphical User Interface for the R Package TIMP. *J. Stat. Softw.* **49**, 1-22 (2012).

41 Kosumi, D. et al. Ultrafast excited state dynamics of fucoxanthin: excitation energy dependent intramolecular charge transfer dynamics. *Phys. Chem. Chem. Phys.* **13**, 10762-10770 (2011).

42 Kusumoto, T. et al. Stark absorption spectroscopy of peridinin and allene-modified analogues. *Chem. Phys.* **373**, 71-79 (2010).

43 Zigmantas, D., Hiller, R. G., Yartsev, A., Sundstrom, V. & Polivka, T. Dynamics of excited states of the carotenoid peridinin in polar solvents: Dependence on excitation wavelength, viscosity, and temperature. *J. Phys. Chem. B* **107**, 5339-5348 (2003).

44 Papagiannakis, E. et al. Use of ultrafast dispersed pump-dump-probe and pump-repump-probe spectroscopies to explore the light-induced dynamics of peridinin in solution. *J. Phys. Chem. B* **110**, 512-521 (2006).

45 Polívka, T., Kerfeld, C. A., Pascher, T. & Sundström, V. Spectroscopic properties of the carotenoid 3 '-hydroxyechinenone in the orange carotenoid protein from the cyanobacterium *Arthrospira maxima*. *Biochemistry* **44** (2005).

46 Pang, Y. & Fleming, G. R. Branching relaxation pathways from the hot S_2 state of 8 '-apo-β-caroten-8 '-al. *Phys. Chem. Chem. Phys.* **12**, 6782-6788 (2010).

47 Redeckas, K., Voiciuk, V., Zigmantas, D., Hiller, R. G. & Vengris, M. Unveiling the excited state energy transfer pathways in peridinin-chlorophyll a-protein by ultrafast multi-pulse transient absorption spectroscopy. *Biochim. Biophys. Acta* **1858**, 297-307 (2017).

48 Niedzwiedzki, D. M., Swainsbury, D. J. K., Canniffe, D. P., Hunter, C. N. & Hitchcock, A. A photosynthetic antenna complex foregoes unity carotenoid-to-bacteriochlorophyll energy transfer efficiency to ensure photoprotection. *Proc. Natl. Acad. Sci. USA* **117**, 6502-6508 (2020).

49 Mendes-Pinto, M. M. et al. Electronic absorption and ground state structure of carotenoid molecules. *J. Phys. Chem. B* **117**, 11015-11021 (2013).

50 Marcolin, G. & Collini, E. Solvent-Dependent Characterization of fucoxanthin through 2D electronic spectroscopy reveals new details on the intramolecular charge-transfer state dynamics. *J. Phys. Chem. Lett.* **12**, 4833-4840 (2021).

51 Slouf, V. et al. Carotenoid charge transfer states and their role in energy transfer processes in LH1-RC complexes from aerobic anoxygenic phototrophs. *J. Phys. Chem. B* **117**, 10987-10999 (2013).

52 Kosumi, D., Horibe, T., Sugisaki, M., Cogdell, R. J. & Hashimoto, H. Photoprotection mechanism of light-harvesting antenna complex from purple bacteria. *J. Phys. Chem. B* **120**, 951-956 (2016).

53 Cohen-Bazire, G., Sistrom, W. R. & Stanier, R. Y. Kinetic studies of pigment synthesis by non-sulfur purple bacteria. *J. Cell. Physiol.* **49**, 25-68 (1957).

54 Nakagawa, K. et al. Electrostatic effect of surfactant molecules on bacteriochlorophyll *a* and carotenoid binding sites in the LH1 complex isolated from *Rhodospirillum rubrum* S1 probed by Stark spectroscopy. *Photosynth. Res.* **95**, 345-351 (2008).

55 Kumble, R., Palese, S., Visschers, R. W., Leslie Dutton, P. & Hochstrasser, R. M. Ultrafast dynamics within the B820 subunit from the core (LH-1) antenna complex of *Rs. rubrum*. *Chem. Phys. Lett.* **261**, 396-404 (1996).

56 Creemers, T. M. H., De Caro, C. A., Visschers, R. W., van Grondelle, R. & Völker, S. Spectral hole burning and fluorescence line narrowing in subunits of the light-harvesting complex LH1 of purple

bacteria. *J. Phys. Chem. B* **103**, 9770-9776 (1999).

57 Lambrev, P. H. et al. Excitation energy trapping and dissipation by Ni-substituted bacteriochlorophyll *a* in reconstituted LH1 complexes from *Rhodospirillum rubrum*. *J. Phys. Chem. B* **117**, 11260-11271 (2013).

58 Fiedor, L. & Scheer, H. Trapping of an assembly intermediate of photosynthetic LH1 antenna beyond B820 subunit: Significance for the assembly of photosynthetic LH1 antenna. *J. Biol. Chem.* **280**, 20921-20926 (2005).

59 Fiedor, L., Akahane, J. & Koyama, Y. Carotenoid-induced cooperative formation of bacterial photosynthetic LH1 complex. *Biochemistry* **43**, 16487-16496 (2004).

60 Duan, S. et al. Hydroquinone redox mediator enhances the photovoltaic performances of chlorophyll-based bio-inspired solar cells. *Commun. Chem.* **4**, 118 (2021).

Supplementary Files

This is a list of supplementary files associated with this preprint. Click to download.

- Yukihira2022SupplementFinal.pdf